







Microelectrode voltage mapping for substrate assessment in catheter ablation of ventricular tachycardia: A dual-center experience

Antonio Dello Russo MD, PhD^{1,2} | Paolo Compagnucci MD^{1,2}  | Marco Bergonti MD³  | Laura Cipolletta MD, PhD² | Quintino Parisi MD, PhD² | Giovanni Volpato MD^{1,2}  | Giulia Santarelli BE² | Michela Colonnelli BE² | Johan Saenen MD, PhD³ | Yari Valeri MD^{1,2}  | Laura Carboni MD⁴ | Procolo Marchese MD⁵  | Marco Marini MD⁶ | Andrea Sarkozy MD, PhD³ | Andrea Natale MD, FHRS^{1,7}  | Michela Casella MD, PhD^{2,8}

¹Department of Biomedical Sciences and Public Health, Marche Polytechnic University, Ancona, Italy

²Cardiology and Arrhythmology Clinic, University Hospital "Ospedali Riuniti", Ancona, Italy

³Department of Cardiology, University Hospital Antwerp, Antwerp, Belgium

⁴Cardiac Surgery Anesthesia and Critical Care Unit, University Hospital "Ospedali Riuniti", Ancona, Italy

⁵Mazzoni Hospital, Ascoli Piceno, Italy

⁶Cardiology Division, University Hospital "Ospedali Riuniti", Ancona, Italy

⁷Texas Cardiac Arrhythmia Institute, Austin, Texas, USA

⁸Department of Clinical, Special and Dental Sciences, Marche Polytechnic University, Ancona, Italy

Correspondence

Paolo Compagnucci, MD, Cardiology and Arrhythmology Clinic, University Hospital "Ospedali Riuniti", Via Tronto 10/a, 60126, Ancona, Italy.
Email: paolocompagnucci1@gmail.com

Abstract

Introduction: The assessment of the ventricular myocardial substrate critically depends on the size of mapping electrodes, their orientation with respect to wavefront propagation, and interelectrode distance. We conducted a dual-center study to evaluate the impact of microelectrode mapping in patients undergoing catheter ablation (CA) of ventricular tachycardia (VT).

Methods: We included 21 consecutive patients (median age, 68 [12], 95% male) with structural heart disease undergoing CA for electrical storm ($n = 14$) or recurrent VT ($n = 7$) using the QDOT Micro catheter and a multipolar catheter (PentaRay, $n = 9$). The associations of peak-to-peak maximum standard bipolar (BV_c) and minipolar (PentaRay, BV_p) with microbipolar ($BV_{\mu\text{Max}}$) voltages were respectively tested in sinus rhythm with mixed effect models. Furthermore, we compared the features of standard bipolar (BE) and microbipolar (μBE) electrograms in sinus rhythm at sites of termination with radiofrequency energy.

Results: $BV_{\mu\text{Max}}$ was moderately associated with both BV_c ($\beta = .85$, $p < .01$) and BV_p ($\beta = .56$, $p < .01$). $BV_{\mu\text{Max}}$ was 0.98 (95% CI: 0.93–1.04, $p < .01$) mV larger than corresponding BV_c , and 0.27 (95% CI: 0.16–0.37, $p < .01$) mV larger than matching BV_p in sinus rhythm, with higher percentage differences in low voltage regions, leading to smaller endocardial dense scar (2.3 [2.7] vs. 12.1 [17] cm^2 , $p < .01$) and border zone (3.2 [7.4] vs. 4.8 [20.1] cm^2 , $p = .03$) regions in microbipolar maps compared to standard bipolar maps. Late potentials areas were nonsignificantly greater in microelectrode maps, compared to standard electrode maps. At sites of VT

Antonio Dello Russo and Paolo Compagnucci contributed equally to this study.

This is an open access article under the terms of the Creative Commons Attribution-NonCommercial License, which permits use, distribution and reproduction in any medium, provided the original work is properly cited and is not used for commercial purposes.

© 2023 The Authors. *Journal of Cardiovascular Electrophysiology* published by Wiley Periodicals LLC.

Disclosures: A. D. R. is a consultant for Abbott Medical. A. N. is a consultant for Biosense Webster, Stereotaxis, and Abbott Medical; has received speaker honoraria/travel from Medtronic, Atricure, Biotronik, and Janssen. The remaining authors declare no conflict of interest.

termination ($n = 14$), μ BE were of higher amplitude (0.9 [0.8] vs. 0.4 [0.2] mV, $p < .01$), longer duration (117 [66] vs. 74 [38] ms, $p < .01$), and with greater number of peaks (4 [2] vs. 2 [1], $p < .01$) in sinus rhythm compared to BE.

Conclusion: microelectrode mapping is more sensitive than standard bipolar mapping in the identification of viable myocytes in SR, and may facilitate recognition of targets for CA.

KEYWORDS

activation mapping, electroanatomical mapping, radiofrequency ablation, substrate mapping, ventricular tachycardia

1 | INTRODUCTION

Catheter ablation (CA) is an important therapeutic option for patients with recurrent ventricular tachycardia (VT) and electrical storm, and the continuous development and clinical validation of novel technology has led to improved procedural and patients' outcomes.^{1,2} Recently, a novel contact-force sensing catheter (QDOT Micro; Biosense Webster) equipped with microelectrodes and thermocouples has been developed and tested in very-high power short duration CA of atrial fibrillation.³ In studies involving swine models of myocardial infarction, microelectrode voltage mapping was shown to have superior sensitivity for the detection of viable myocardium compared to standard bipolar mapping.⁴⁻⁶ As of today, however, we are lacking information on the clinical value of microelectrode voltage mapping among human subjects undergoing CA for VT. The aim of the present study is to report on the preliminary clinical experience with microelectrode mapping as compared to standard bipolar mapping in the setting of VT CA.

2 | METHODS

2.1 | Patients

Consecutive patients with structural heart disease undergoing CA for ES or recurrent VT at two European referral institutions (University Hospital "Ospedali Riuniti" and University Hospital of Antwerp) between September 2021 and March 2022 were retrospectively included in this study. Left ventricular (LV) aneurysms were defined as circumscribed, thin-walled fibrous, noncontractile outpouchings of the ventricle, identified at preprocedural transthoracic echocardiogram.⁷ The study protocol was approved by the institutional review board, and each patient provided his/her written informed consent.

2.2 | Electrophysiology procedure

The electrophysiology procedure was performed under general anesthesia. The type of approach (endocardial vs. epi-endocardial)

was chosen according to VT morphology, preprocedural imaging, and the type of structural heart disease (ischemic vs. nonischemic). Intracardiac echocardiography (ICE) was used in each case, to rule out intracardiac thrombosis, monitor for procedural complications in real-time, and verify catheter's position and catheter-tissue contact. In case of epi-endocardial approach, the epicardium was preliminary accessed with a posterior subxiphoid puncture, using the Sosa technique and a deflectable sheath (Agilis EPI; Abbott). The access route (transseptal vs. retrograde aortic) to the LV endocardium was chosen according to operators' preference, preprocedural imaging, and the presumed site of origin of VT. Unfractionated heparin was administered during LV endocardial steps of procedures, to achieve an activated clotting time ≥ 300 s.²

2.3 | Electroanatomical mapping and electrophysiology study

Electroanatomical reconstructions of the LV endocardium and/or epicardium were obtained with the CARTO3 version7 mapping system (Biosense Webster). Substrate mapping was performed in sinus rhythm with the contact-force sensing catheter with microelectrodes and thermocouples (QDOT Micro; Biosense Webster). The QDOT Micro catheter integrates a standard distal bipole (between the 3.5 mm tip and a 1 mm spaced 1 mm ring) recording standard bipolar electrograms with 3 tip microelectrodes (0.167 mm² wide, 1.755 mm spaced), each recording microbipolar electrograms at 60° angles to other microbipolar electrograms and perpendicular to the standard bipolar electrogram. Only points with adequate catheter-tissue contact (>3 g) were acquired; for each point, the system automatically acquired the standard bipolar electrogram and the microbipolar electrogram with the highest amplitude, to correct for wavefront propagation direction.⁴⁻⁶ Operators were also allowed to use a multipolar catheter with 5 splines, each with 4 1 mm wide electrodes with 2-6-2 mm spacing (PentaRay; Biosense Webster), recording bipolar electrograms between each 2 mm spaced electrogram pair (minibipolar electrograms). Catheter-tissue contact was verified with fluoroscopy, signal characteristics, and ICE, and points acquired with the PentaRay catheter were filtered using the tissue

proximity indication (Biosense Webster) algorithm. In patients with LV aneurysms, ICE was used to delineate the aneurysms' three-dimensional geometry and integrate it with electroanatomical maps, using the Cartosound module (Biosense Webster).

Conventional cutoffs were used to define dense scar regions (<0.5 mV in the endocardium, <0.3 mV in the epicardium) and border zones (0.5–1.5 mV in the endocardium, 0.3–0.8 mV in the epicardium) in both the standard bipolar, minibipolar, and microbipolar maps.^{8,9} At the same time, myocardial regions showing late-fragmented potentials were annotated.

After substrate mapping, programmed electrical stimulation (PES) was performed from multiple RV/LV sites using a minimum of two cycle drive lengths (600 and 400 ms), with up to three extrastimuli, until VT induction, ventricular refractoriness, or coupling interval of 200 ms were reached.

2.4 | CA

In case of hemodynamically tolerated VT induction, activation, and entrainment mapping were performed with the QDOT Micro catheter, and radiofrequency energy was delivered in regions showing mid-diastolic electrograms and good entrainment (i.e., entrainment with concealed fusion and [postpacing interval–tachycardia cycle length] <30 ms), targeting VT termination. In case of hemodynamically unstable VT, electrical cardioversion was performed. After VT termination, substrate homogenization was completed, targeting elimination of all abnormal late/fragmented electrograms.⁹ Radiofrequency energy was delivered in a temperature-controlled fashion (QMODE™; Biosense Webster), power setting 40–50 W, and recommended contact force 5–20 g; the choice of power, contact force, and duration of radiofrequency energy delivery were left at the discretion of operators. An automated lesion tagging module (Visitag Module; Biosense Webster) was used to mark the location of each radiofrequency lesion with the following settings: catheter stable for at least 3 s within a 3 mm range and at least 3 g of contact force for 25% of the stability time.^{10,11} For each case, we recorded the number of Visitags, minimum and maximum power, as well as maximum and mean ablation index values, as previously described.^{10,12} In inducible patients, PES was repeated at end procedure; complete procedural success was defined as absence of any VT inducibility; partial procedural success was defined as nonclinical VT inducibility; procedural failure was defined as persistent inducibility of clinical VT.

2.5 | Postprocedural case/electrogram analysis and patient follow-up

After the procedure, CARTO files were deidentified and sent for analysis to a core laboratory at the Marche Polytechnic University. For each patient, substrate assessment with standard bipolar (QDOT

Micro), minibipolar (PentaRay), and microbipolar (QDOT Micro) mapping were compared, by measuring the extension of dense scar and border zone regions, as well as the extension and location of areas displaying late potentials with each mapping approach. For every mapping location, the maximum peak-to-peak amplitude of microbipolar electrograms was compared with both standard bipolar and corresponding minibipolar (by matching mapping points acquired with the QDOT Micro catheter with those acquired with the PentaRay catheter within 1 mm) electrograms. Furthermore, when VT could be terminated with RF energy delivery, the characteristics of the standard bipolar and microbipolar electrogram in sinus rhythm at the termination point were assessed and compared, by measuring maximum peak-to-peak amplitude, total electrogram duration, and the number of electrogram peaks, as evaluated before any RF energy was delivered.

Each patient was followed-up by means of implantable defibrillator remote monitoring to identify VT recurrences; furthermore, telephonic follow-up was performed to assess for late complications.

2.6 | Statistics

Categorical variables are presented as count (percentage), whereas continuous quantitative variables are reported as mean ± standard deviation or median (interquartile range), as appropriate for normally and non-normally distributed variables, respectively. The correlation of microbipolar and standard bipolar or minibipolar electrogram amplitude was explored with scatter plots and assessed with a mixed effect model, by clustering data from all patients and accounting for the patient and the mapping approach (endocardial vs. epicardial) as independent random effects. Bland–Altman plots were used to evaluate agreement between microbipolar and standard bipolar or minibipolar electrogram amplitude. Differences in the extension of dense scar, border zone regions, and electrogram characteristics at termination sites in bipolar and microbipolar maps were assessed with repeated measures ANOVA, paired t, or Wilcoxon tests, as appropriate. The Bonferroni correction was used to account for multiple comparisons. All statistical analyses were performed with the software RStudio; *p* values < .05 were considered statistically significant.

3 | RESULTS

The clinical characteristics of the patients at baseline are presented in Table 1. In brief, the study population included 21 patients (age, 68 [12] years; male sex, *n* = 20, 95%) who underwent CA for ES (*n* = 14, 67%) or VT (*n* = 7, 33%). Prior myocardial infarction was the most common underlying substrate (*n* = 12, 57%), while LV aneurysms were noted in 10 patients (48%), mainly in patients with ischemic cardiomyopathy (*n* = 7).

TABLE 1 Characteristics of the patients at baseline.

	Overall (n = 21)
Age—years (IQR)	68 (12)
Male sex—n (%)	20 (95)
NYHA functional class—median (IQR)	2 (0)
BMI—kg/m ² —(SD)	28.6 (5.4)
Arrhythmia type	
Electrical storm—n (%)	14 (66.7)
Recurrent paroxysmal VT—n (%)	7 (33.3)
Substrate	
Prior myocardial infarction—n (%)	12 (57.1)
Dilated cardiomyopathy—n (%)	3 (14.3)
Congenital heart disease—n (%)	2 (9.5)
Arrhythmogenic cardiomyopathy—n (%)	1 (4.8)
Cardiac sarcoidosis—n (%)	1 (4.8)
Cardiac amyloidosis—n (%)	1 (4.8)
Hypertrophic cardiomyopathy—n (%)	1 (4.8)
Left ventricular aneurysm—n (%)	10 (47.6)
Apical aneurysm—n (%)	5 (23.8)
Inferior-lateral aneurysm—n (%)	4 (19.1)
Inferior-septal aneurysm—n (%)	1 (4.8)
Left ventricular ejection fraction—% (SD)	37 (11)
Left ventricular end diastolic volume—mL (SD)	176 (51)
Atrial fibrillation—n (%)	8 (38.1)
Diabetes mellitus—n (%)	1 (4.8)
Systemic arterial hypertension—n (%)	13 (61.9)

Abbreviations: BMI, body mass index; NYHA, New York heart association; VT, ventricular tachycardia.

Procedural characteristics are presented in Table 2. The procedural approach was endocardial, epi-endocardial, and epicardial in 18 (86%), 2 (10%), and 1 (5%) patient, respectively. Six subjects (29%) had previously undergone CA of VT; in one of them, the first procedure was endocardial, while the second epicardial; in the remaining five, all procedures were endocardial. The median procedural duration was 198 (46) min, while the median mapping time was 25 (39) min. The PentaRay catheter was used in 9 patients (43%). The average numbers of points collected with the QDOT Micro catheter were 599 (306) and 883 ± 346 in the endocardium and epicardium, respectively, while the average numbers of points collected with the PentaRay catheter were 1049 ± 840 and 3385 ± 2689 in the endocardium and epicardium, respectively. A total of 34 VTs were induced (2 ± 1 per patient), of which 15 (44%, 1 [1] per patient) could be completely mapped. Radiofrequency energy was delivered for a mean of 16 ± 6 min, with minimum power set at 40 (10) W, and maximum power set at 50 (10) W.

TABLE 2 Procedural characteristics.

	Overall (n = 21)
First procedure—n (%)	15 (71.4)
Second procedure—n (%)	5 (23.8)
Third procedure—n (%)	1 (4.8)
Procedural approach	
Endocardial—n (%)	18 (85.7)
Epi-endocardial—n (%)	2 (9.5)
Epicardial—n (%)	1 (4.8)
Endocardial access to the left ventricle	20 (95.2)
Single transseptal puncture—n (%)	18 (85.7)
Retrograde aortic—n (%)	3 (14.3)
Number of induced VT—mean (SD)	2 (1)
Zero—n (%)	4 (19.1)
One—n (%)	6 (28.6)
Two—n (%)	6 (28.6)
Three—n (%)	4 (19.1)
Four—n (%)	1 (4.8)
Number of mapped VT—median (IQR)	1 (1)
Zero—n (%)	6 (28.6)
One—n (%)	15 (71.4)
Procedural duration—min (IQR)	198 (46)
Mapping duration—min (IQR)	25 (39)
Catheters used	
QDOT Micro™—n (%)	21 (100)
PentaRay™—n (%)	9 (42.9)
Number of mapping points	
QDOT Micro, endocardium—n (IQR)	599 (306)
QDOT Micro, epicardium—n (SD)	883 (346)
PentaRay, endocardium—n (SD)	1049 (840)
PentaRay epicardium—n (SD)	3385 (2689)
Late potentials—n (%)	19 (90.5)
Late potentials area in standard bipolar mapping—cm ² (SD)	4.2 (4.3)
Late potentials area in microelectrode mapping—cm ² (SD)	4.5 (4.2)
Total radiofrequency time—min (SD)	16 (6)
Median area covered by ablation—cm ² (IQR)	13.2 (7.1)
Ablation settings	
Minimum power—W (IQR)	40 (10)
Maximum power—W (IQR)	50 (10)
Number of VISITAGs™, endocardium—n (SD)	39 (20)
Number of VISITAGs™, epicardium—n (SD)	37 (12)

(Continues)

TABLE 2 (Continued)

	Overall (n = 21)
Mean time spent at each ablation site—s (SD)	26 (14)
Maximum ablation index, endocardium—n (SD)	612 (67)
Mean ablation index, endocardium—n (IQR)	458 (82)
Maximum ablation index, epicardium—n (SD)	611 (6)
Mean ablation index, epicardium—n (SD)	500 (57)
VT termination with RF delivery—n (%)	14 (66.7)

Abbreviations: IQR, interquartile range; VT, ventricular tachycardia.

3.1 | Substrate analysis by simultaneous recordings of standard bipolar and microbipolar electrograms

Standard bipolar and microbipolar electrograms were recorded at 8888 locations, 7628 of which in the endocardium, and the remaining in the epicardium. The peak-to-peak amplitudes of standard bipolar and maximum microbipolar electrograms were positively related at regression analysis, but with suboptimal goodness of fit ($\beta = .85$, intercept = 0.83, $R^2 = 0.43$, $p < .01$; Figure 1, panel A). Maximum microbipolar electrogram amplitude (average, 2.85 ± 3.36 mV) was greater than the corresponding standard bipolar electrogram amplitude (average, 1.87 ± 2.29 mV) by 0.98 (95% CI: 0.93–1.04, $p < .01$) mV, and the average percentage difference was $39.5 \pm 82\%$. When separately analyzing electrogram amplitude inside LV aneurysms, maximum microbipolar electrogram amplitude exceeded standard bipolar electrogram amplitude by 1.22 [95% CI: 0.96–1.48, $p < .01$] mV (Figure 2). Although the absolute difference between microbipolar and standard bipolar electrogram amplitude was smaller in areas with standard bipolar voltage ≤ 1.5 mV compared to areas with standard bipolar voltage > 1.5 mV (0.7 vs. 1.4 mV, $p < .01$), the percentage difference between microbipolar and bipolar electrograms was significantly higher in regions with standard bipolar voltage ≤ 1.5 mV (54.7% vs. 14.3%, $p < .01$). Supporting Information: Figure 1 shows the Bland–Altman plots of the absolute and percentage differences between microbipolar and standard bipolar electrograms.

Of note, considering the standard bipolar voltage criteria for dense scar and border zone regions in the endocardium (dense scar, < 0.5 mV; border zone, 0.5–1.5 mV) and in the epicardium (dense scar, < 0.3 mV; border zone, 0.3–0.8 mV), microbipolar mapping led to voltage category reclassification in 42.2% of mapping points in the endocardium and in 35.8% of mapping points in the epicardium (Figure 3; overall reclassification rate, 41.3%), mainly involving dense scar and border zone regions, and particularly pronounced inside LV aneurysms (57.8% reclassification rate, Figure 3, panel C).

Comparing the extension of dense scar and border zone regions in bipolar and microbipolar endocardial and epicardial maps, we found that both were significantly smaller in microbipolar maps than in bipolar maps in the endocardium ($p = .0007$ and $p = .03$, respectively, Table 3, Central Illustration).

In the analysis of microbipolar and bipolar electrogram amplitude in nonischemic cardiomyopathies (Supporting Information: Table 1), we found a greater absolute difference between corresponding microbipolar and standard bipolar electrogram amplitudes in arrhythmogenic cardiomyopathy and cardiac sarcoidosis in the endocardium, and in hypertrophic cardiomyopathy in the epicardium.

We also found that the locations of late potentials were always concordant between standard electrode and microelectrode mapping, and that the extension of late potentials areas was non-significantly larger with microelectrode mapping ($4.5 [4.2]$ vs. $4.2 [4.3]$ cm², $p = .099$; Table 2, Figure 4).

3.2 | Substrate analysis by simultaneous recordings of minibipolar and microbipolar electrograms

Matching minibipolar and microbipolar electrograms were available at 1532 mapping points, 749 of which in the endocardium. Microbipolar and minibipolar electrograms' amplitudes were positively associated, but with moderate fit ($\beta = .56$, intercept = 1.19, $R^2 = 0.46$, $p < .01$; Figure 1, panel B). Overall, microbipolar electrogram amplitude (average, 1.73 ± 2.35 mV) was greater than corresponding minibipolar electrogram amplitude (average, 1.47 ± 1.94 mV; absolute difference, 0.27 [95% CI: 0.16–0.37, $p < .01$]; percentage difference, $16.7 \pm 97.5\%$; Figure 5). Both the absolute and the percentage differences between microbipolar and minibipolar electrograms amplitude were higher in regions with minibipolar voltage ≤ 1.5 mV compared to other regions (0.49 vs. -0.26 mV, $p < .01$, and 35% vs. -28.3% , $p < .01$). Bland–Altman plots of absolute and percentage differences between microbipolar and minibipolar electrogram amplitudes are shown in Supporting Information: Figure 1. Voltage category reclassification using conventional voltage criteria for dense scar and border zone regions with microbipolar versus minibipolar mapping occurred at 54.9% and 39.2% of mapped locations in the endocardium and epicardium, respectively (Supporting Information: Figure 1; overall reclassification rate, 46.9%). The comparisons of the extension of dense scar/border zone regions and of late potentials areas among standard electrode, minielectrode, and microelectrode maps are reported in the Supporting Information: Tables 2 and 3, respectively.

3.3 | Analysis of bipolar and microbipolar electrograms at VT termination sites

Of the 15 mapped VT (cycle length, 419 ± 90 ms), 14 (93%) could be terminated with radiofrequency energy delivery in regions showing diastolic electrograms. In 8 cases, VT termination occurred with radiofrequency energy delivery in the endocardium, inside LV aneurysms (Figure 6, Central Illustration, Supporting Information: video).

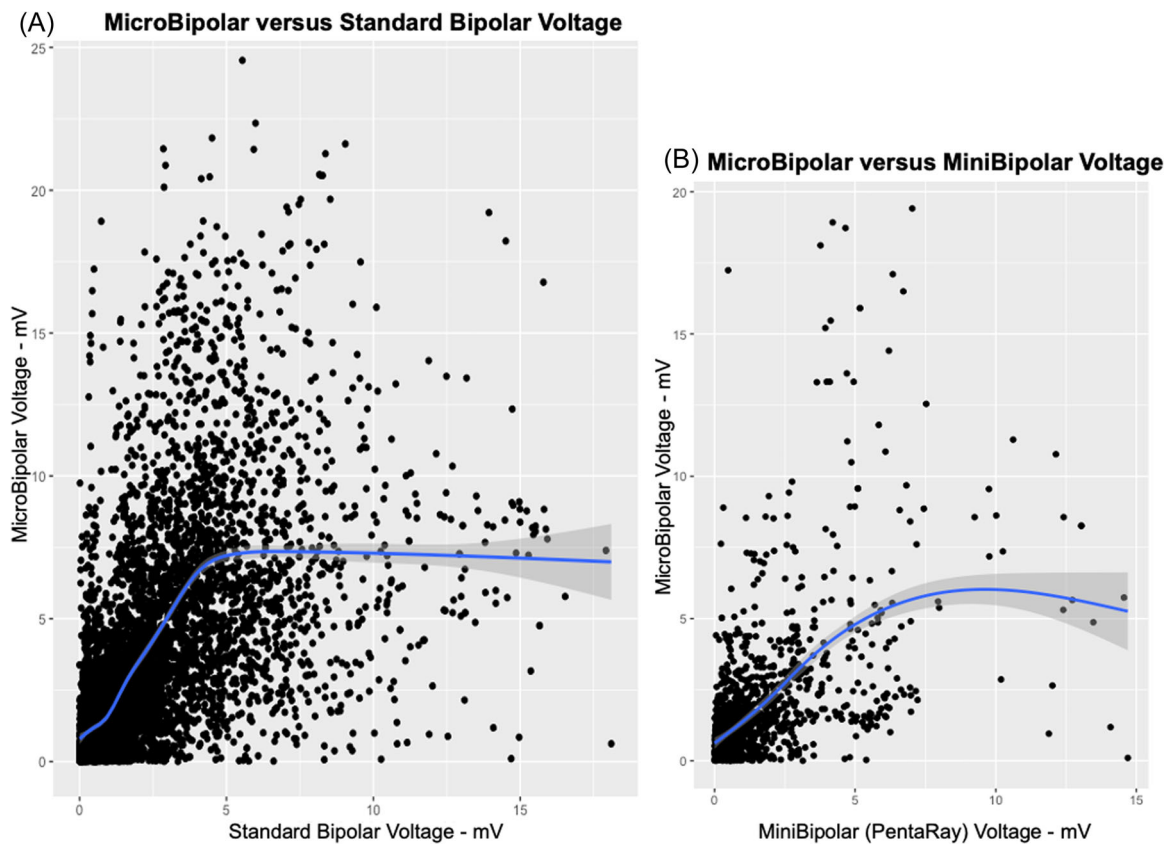


FIGURE 1 The amplitude of maximum peak-to-peak microbipolar electrograms versus the amplitude of standard peak-to-peak bipolar or minibipolar electrograms. (A) Comparison of the amplitude of microbipolar and standard bipolar electrograms. (B) Comparison of the amplitude of microbipolar and minibipolar electrograms. The blue curves are “smooth” locally weighted least squares regressions, with polynomial degree = 2, and span of $\alpha = .75$. The gray areas surrounding the regression curve represent the 95% confidence intervals.

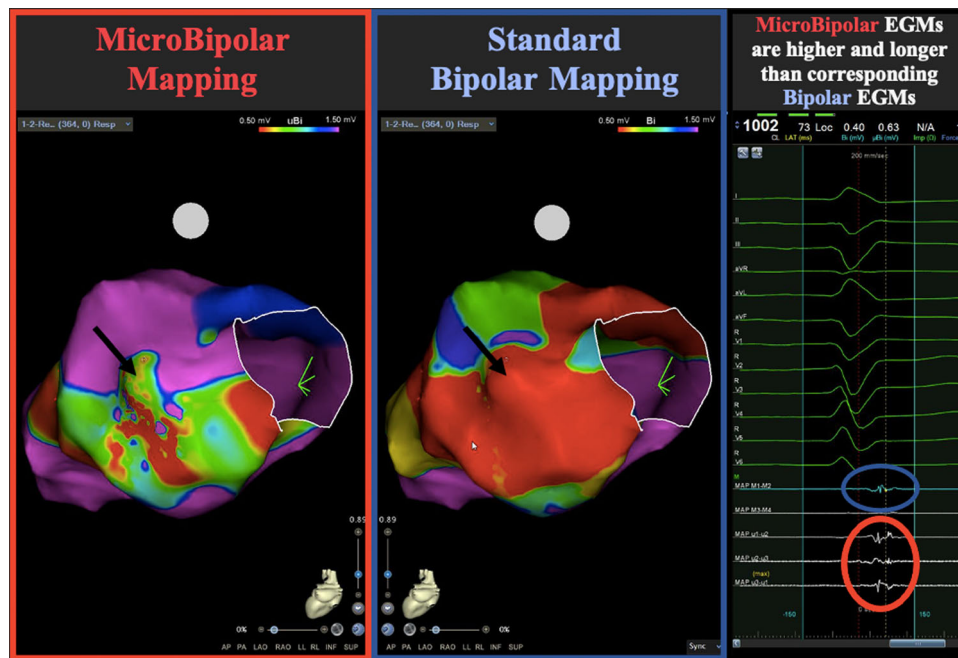


FIGURE 2 Comparison of standard bipolar and microbipolar endocardial mapping. The left panel shows the microbipolar voltage map in a case of postinfarction inferior-lateral left ventricular aneurysm, while the central panel shows the corresponding standard bipolar map using the same voltage cutoffs. Note that the microbipolar map reveals viable myocardium in the region of the aneurysm (black arrow). The right panel shows bipolar and corresponding microbipolar electrograms; note that microbipolar electrograms are higher in amplitude and longer.

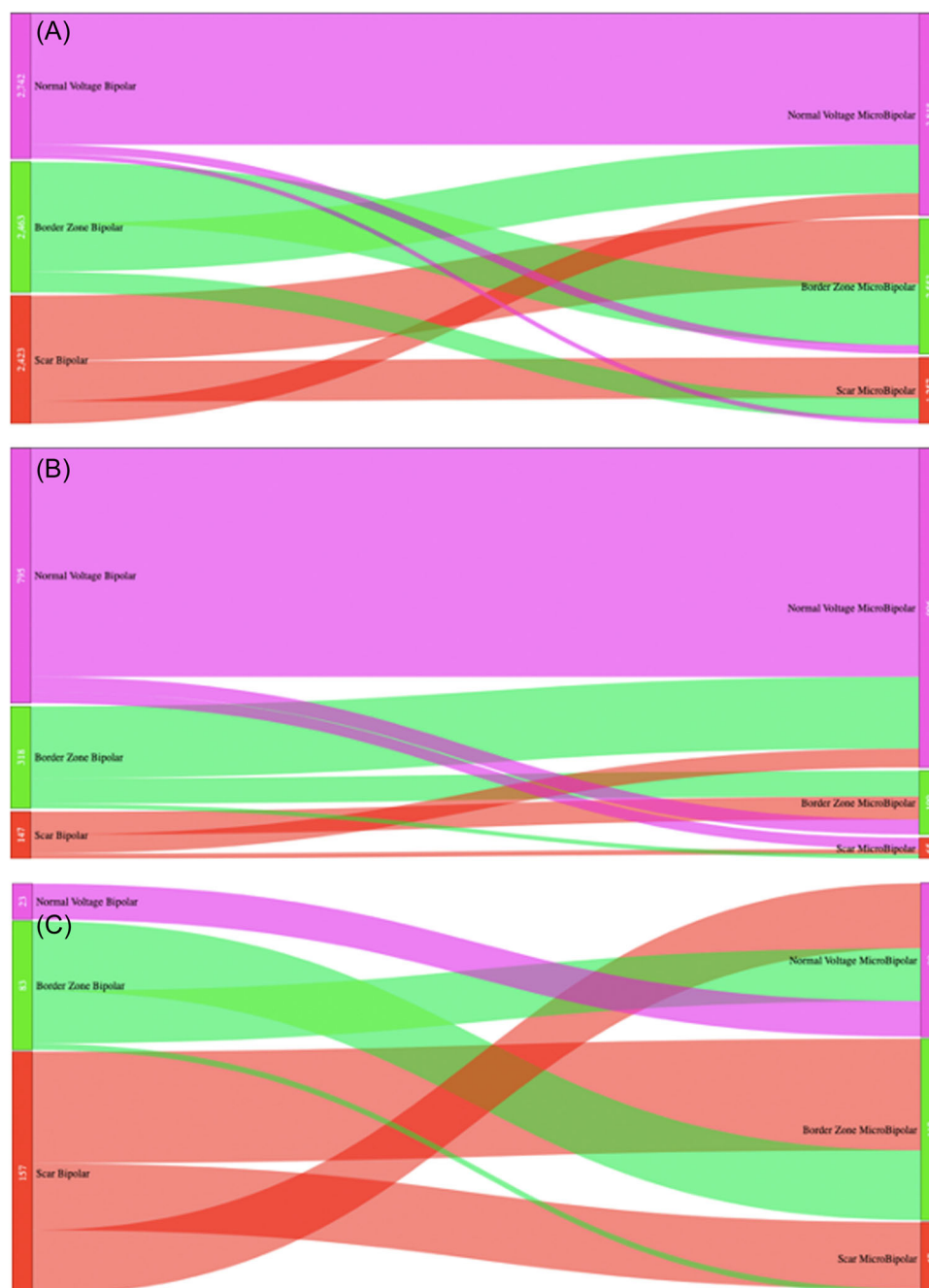


FIGURE 3 Voltage category reclassification from standard bipolar to microbipolar mapping using standard voltage cutoffs. Sankey diagrams schematically representing voltage category reclassification from standard bipolar (left) to microbipolar mapping (right) for each mapping location in the endocardium (A), in the epicardium (B), and inside left ventricular aneurysms (C).

We assessed and compared the characteristics of bipolar and microbipolar electrograms at VT termination points in sinus rhythm, and found that microbipolar electrograms were of significantly higher amplitude (0.9 [0.8] vs. 0.4 [0.2] mV, $p = .0006$, respectively), longer duration (117 [66] vs. 74 [38], $p = .001$), and had a significantly greater number of peaks (4 [2] vs. 2 [1], $p = .0009$; [Central Illustration](#)). Minibipolar electrograms at termination points were available in 5 patients; the comparison among standard bipolar, minibipolar, and microbipolar electrograms at sites of VT termination are shown in Supporting Information: Table 4.

3.4 | Procedural efficacy, complications, and follow-up

Of the 17 inducible patients (81%), complete acute success (absence of any VT inducibility by PES at end procedure) was achieved in 13, while partial procedural success (inducibility of only nonclinical VT at end procedure) was obtained in 3. We observed no early or late procedural complications (including no steam pops), and after a median follow-up of 4 (4) months, there were no VT recurrences.

TABLE 3 Comparison of the extension of dense scar and border zone between standard bipolar and microbipolar mapping, in the endocardium and epicardium.

		Standard Bipolar mapping	MicroBipolar mapping	p
Endocardium (n = 20)	Dense scar area (<0.5 mV) cm ²	12.1 (17)	2.3 (2.7)	.0007
	Border zone area (0.5–1.5 mV) cm ²	4.8 (20.1)	3.2 (7.4)	.03
Epicardium (n = 3)	Dense scar area (<0.3 mV) cm ²	11.5 (10)	0.2 (0.3)	.18
	Border zone area (0.3–0.8 mV) cm ²	5.5 (3.6)	3.2 (5.2)	.43

Note: Results are presented as mean (standard deviation) or median (interquartile range), as appropriate. p Values are calculated with paired-sample Student t or Wilcoxon rank-sum test, as appropriate. Bold values are statistically significant.

CENTRAL ILLUSTRATION

Microbipolar electrograms are significantly higher than both corresponding standard bipolar and minibipolar electrograms in sinus rhythm, leading to significantly smaller low-voltage regions in endocardial maps. Furthermore, microbipolar electrograms at sites of ventricular tachycardia termination are longer, more fragmented, and of higher amplitude than standard bipolar electrograms in sinus rhythm.

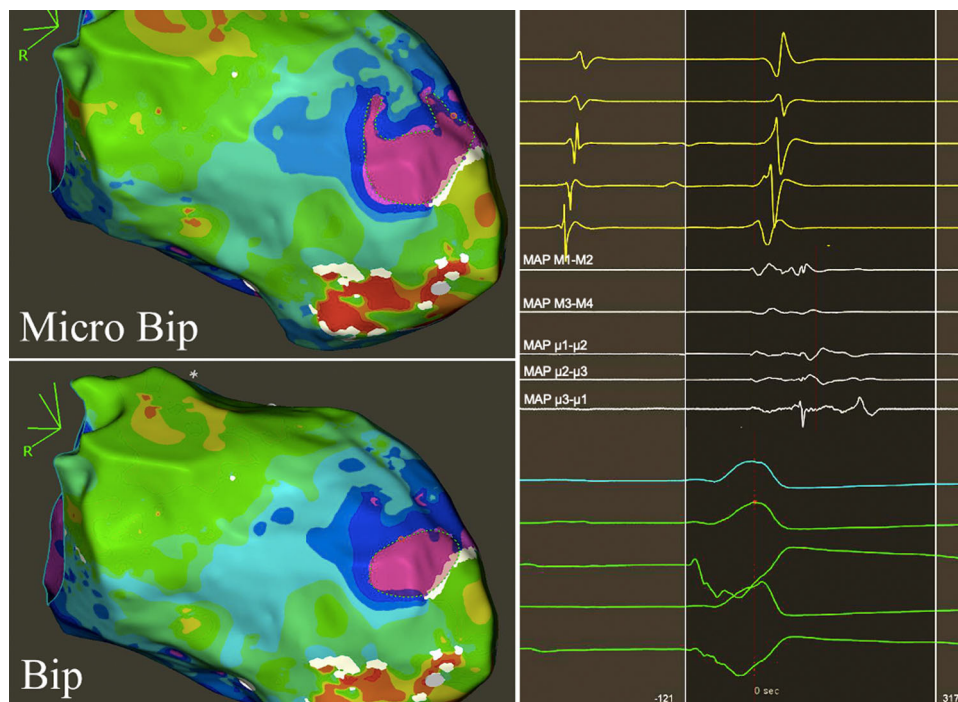
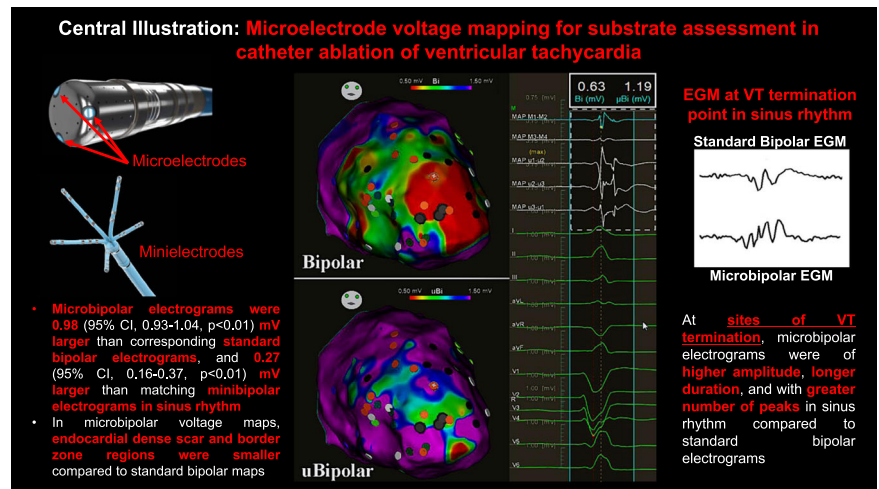


FIGURE 4 Comparison in the extension of late potentials areas between standard bipolar (Bip) and microelectrode (Micro Bip) mapping. Note that in this patient with prior anterior myocardial infarction, late potentials are colocalized in the two maps, although the extension of the late potentials area is slightly greater in the microelectrode map (upper panel).

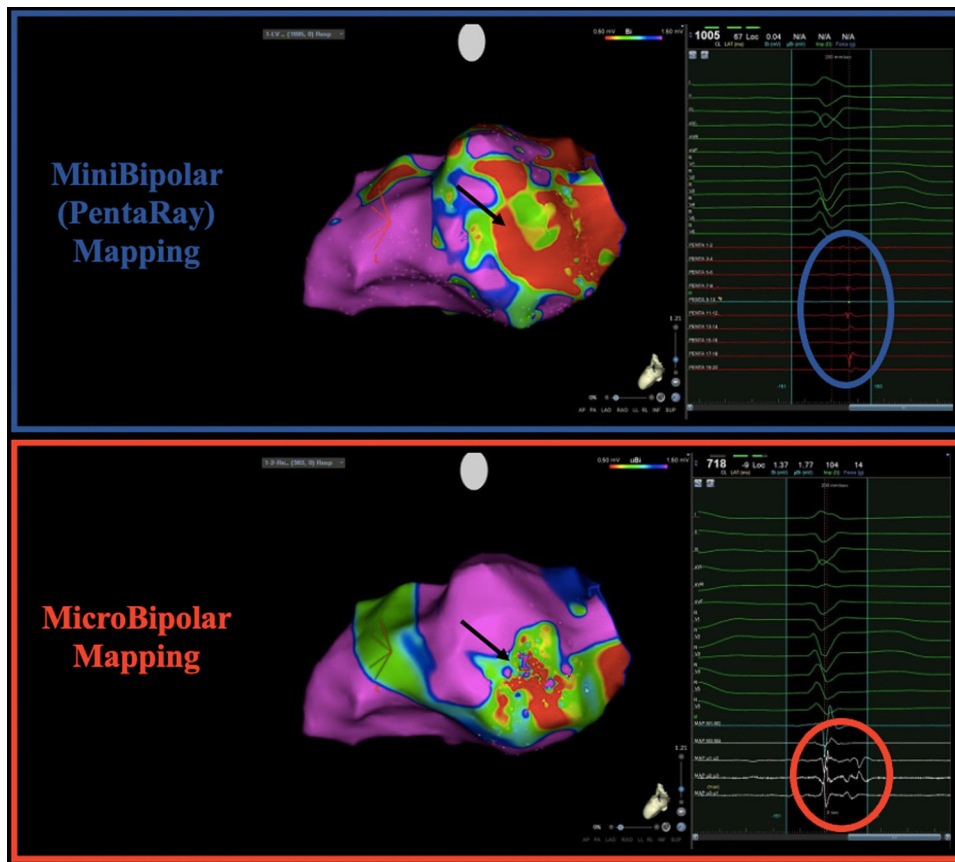


FIGURE 5 Comparison of minibipolar (PentaRay) and microbipolar mapping. The upper panel shows the minibipolar (PentaRay) endocardial voltage map, revealing scarring of the basal posterior and inferior walls of the left ventricle. In the inferior panel, the microbipolar map using the same voltage cutoffs shows a more heterogeneous substrate in the same region, with clearer visualization of late potentials.

4 | DISCUSSION

We present the preliminary experience with the novel QDOT Micro catheter in substrate mapping and CA of VT in patients with structural heart disease. The findings of our study have several implications for clinicians.

- (1) Microelectrode mapping, by capturing electrical information from submillimetric electrodes, allows the visualization of higher electrograms in low bipolar voltage areas in sinus rhythm, as a result of the more sensitive detection of viable and electrically non-inert subendocardial (or subepicardial) myocardial tissue.^{5,6,13} This tissue, while potentially overlooked with the use of conventional bipolar electrodes and even with multipolar catheters, as the PentaRay, may in turn represent a critical component of the arrhythmia circuitry and a fundamental target for ablation.¹³ This finding translates into smaller but better characterized target zones for substrate-based CA of VT.
- (2) At sites of VT termination (i.e., presumed VT isthmuses), microelectrode mapping in sinus rhythm reveals higher, longer, and more fractionated electrograms, highlighting the potential pathogenicity of the regions.

- (3) Using standard voltage cutoffs, a high proportion of mapping points may change their voltage category with microelectrode mapping compared to standard bipolar mapping (41.3% reclassification rate) or minibipolar mapping (46.9% reclassification rate), underscoring the need to adapt voltage cutoffs according to recording electrode dimensions.

4.1 | Conventional electrodes, minielectrodes, microelectrodes, and the detection of electrically viable myocardium

The choice of specific voltage cutoffs to discriminate dense scar and border zone regions from normal-voltage myocardium has crucial consequences at the time of CA of VT in patients with structural heart disease.¹³ In fact, low-voltage regions are also commonly associated with slowing of conduction and, therefore, usually contain critical VT circuit components, thus representing targets for CA.¹³ On the other hand, CA should be avoided in areas displaying normal voltages, where ablation-induced injury may result in potentially harmful conduction slowing.

Unfortunately, the available data to categorize myocardial segments according to their peak-to-peak voltage amplitude were

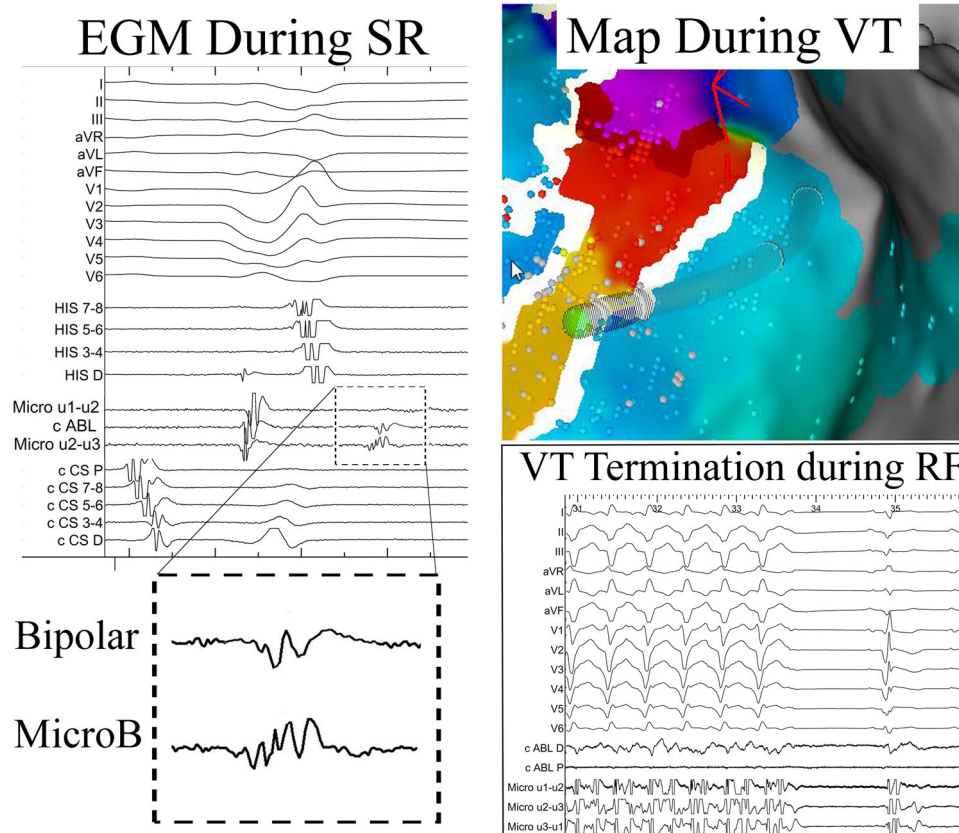


FIGURE 6 Standard bipolar and microbipolar electrogram characteristics in sinus rhythm at a site of ventricular tachycardia (VT) termination. Note that the microbipolar electrogram is longer, with more peaks, and of slightly higher amplitude compared to the standard bipolar electrogram. EGM, electrogram; MicroB, microbipolar; RF, radiofrequency; SR, sinus rhythm; VT, ventricular tachycardia.

derived in 1980s studies involving patients without structural heart disease,¹⁴ using widely spaced (5–10 mm) electrodes.^{14,15} Even more recent reports on the correlation between electrogram voltage and myocardial fibrosis, as assessed by whole heart histology¹⁶ or cardiac magnetic resonance imaging,¹⁷ are limited by the use of conventional mapping catheters with 3.5 mm tip electrode, 1 mm ring electrode, and 2 mm interelectrode spacing.^{16,17} Accumulating evidence is supporting the concept that using smaller electrodes may allow the detection of higher amplitude signals,^{4–6} which may translate into the need to dynamically adjust voltage cutoffs in microelectrode maps,^{4,5} but the clinical impact of this phenomenon has not been quantified in humans and needs to be investigated further. In fact, all data regarding substrate-based ablation for VT have been acquired with a standard bipolar configuration, and we cannot exclude that microbipolar mapping may have a deep impact on the procedural approach to substrate homogenization, pushing operators toward less extensive ablation lesions sets directed to more limited regions of interest.¹⁰

As opposed to prior swine models of myocardial infarction,⁶ we found higher percentage spread between maximum microbipolar and maximum bipolar electrogram amplitudes in lower voltage regions.⁶ This finding underlines how critical the information captured by microelectrode mapping may be in the identification of surviving

bundles of myocytes inside dense scar regions as defined by standard bipolar mapping voltage criteria, especially in the context of VT CA in patients with ischemic cardiomyopathy. In fact, the widespread adoption of early percutaneous coronary intervention in myocardial infarction has led to reduced size and increased heterogeneity of myocardial scar, whose electrical properties may be better characterized by using submillimetric microelectrodes.¹³ Furthermore, the three-dimensional arrangement of the three 60°-angled microelectrodes and the automatic selection of the electrogram with the highest peak-to-peak voltage allows compensation of the variable relationship between catheter-tissue contact angle and wavefront propagation direction, which may be particularly relevant in scarred myocardial segments, where complex patterns of wavefront propagation (including “zigzag” course of activation)¹⁸ have been described.^{5,19} Although our study had limited statistical power, we found that the extension of areas with late potentials was non-significantly larger with microelectrode mapping, and we may speculate that microelectrode mapping may become an important mapping modality for the characterization of late/fragmented, low-voltage electrograms.

Based on our findings (Supporting Information: Table 1), we cannot exclude that the differential diagnostic value of microbipolar mapping compared to standard bipolar mapping may be substrate-

specific in nonischemic cardiomyopathies, a finding that deserves further study.

4.2 | Impact of microelectrode mapping and temperature-controlled ablation in patients with LV aneurysms

Ventricular aneurysms are commonly associated with recurrent VT due to reentry involving surviving myocytes inside the aneurysm or at its edge.^{7,20-22} In the subset of patients with LV aneurysms in our study ($n = 10$), standard bipolar voltage mapping in sinus rhythm showed dense scar electrograms in 59.7% of mapping locations inside the aneurysm (Figure 2, panel C). However, microelectrode mapping allowed the detection of significantly higher voltages in the same locations. Of note, in 80% of patients in this subset, we were able to terminate VT with radiofrequency energy delivery inside the aneurysm; furthermore, the analysis of sinus rhythm electrograms at termination sites showed longer and more complex electrograms with microelectrode mapping, compared to standard bipolar mapping. We hypothesize that these results represent an enhancement of what was previously shown with ultra high-density mapping of postinfarction LV scar,²³ in that microelectrode mapping may facilitate visualization of arrhythmogenic low amplitude electrograms within scarred regions.

As an important corollary, the availability of 6 thermocouples and adjustable irrigation flow rate allowed optimized temperature-controlled ablation,³ leading to absence of steam pops or other procedural complications even in the challenging context of LV aneurysms, in which the very limited wall thickness may facilitate pericardial effusions and myocardial perforation, especially when using high radiofrequency energy power.

4.3 | Limitations

In our study, not all patients underwent mapping with the PentaRay catheter, and we were not able to collect standard bipolar, minibipolar, and microbipolar electrogram at every mapping point, due to slight differences in the mapped LV geometry. However, the large number of collected points allowed us to draw statistically solid conclusions on the relationships between microbipolar and either standard bipolar or minibipolar electrograms. The present study has a limited sample size, a short follow-up, and mainly included male subjects. Larger numbers of patients, longer follow-ups, and more female patients need to be studied before we may assess the safety and efficacy of CA of VT with the novel QDOT Micro catheter. Nonetheless, to our knowledge, this is the largest report on the use of the QDOT Micro catheter in human subjects undergoing substrate mapping and CA of VT, the only other report being specifically focused on the assessment of local abnormal ventricular activity with the QDOT Micro catheter in 4 patients.²⁴ Finally, we did not analyze

whether microelectrodes may be of help in activation mapping of VT, and this is a currently unanswered research question.

5 | CONCLUSIONS

Microelectrode mapping allows detection of higher voltage electrograms compared to standard bipolar mapping, a phenomenon which mostly impacts on the electrophysiological characterization of scarred regions. We believe that this preliminary experience may pave the way for further assessments of this new technology in the so far less explored ventricular milieu.

ACKNOWLEDGEMENTS

Open Access Funding provided by Universita Politecnica delle Marche within the CRUI-CARE Agreement.

DATA AVAILABILITY STATEMENT

The data that support the findings of this study are available on request from the corresponding author, P. C.

ORCID

Paolo Compagnucci  <https://orcid.org/0000-0003-1924-6548>

Marco Bergonti  <http://orcid.org/0000-0001-9864-1938>

Giovanni Volpato  <http://orcid.org/0000-0002-5593-3591>

Yari Valeri  <http://orcid.org/0000-0002-0454-0739>

Procolo Marchese  <http://orcid.org/0000-0002-2677-9214>

Andrea Natale  <http://orcid.org/0000-0002-5487-0728>

REFERENCES

1. Compagnucci P, Volpato G, Falanga U, et al. Recent advances in three-dimensional electroanatomical mapping guidance for the ablation of complex atrial and ventricular arrhythmias. *J Interv Card Electrophysiol*. 2021;61(1):37-43.
2. Cronin EM, Bogun FM, Maury P, et al. 2019 HRS/EHRA/APHS/LAHS expert consensus statement on catheter ablation of ventricular arrhythmias. *EP Europace*. 2019;21(8):1143-1144.
3. Reddy VY, Grimaldi M, De Potter T, et al. Pulmonary vein isolation with very high power, short duration, temperature-controlled lesions. *JACC: Clin Electrophysiol*. 2019;5(7):778-786.
4. Leshem E, Tschabrunn CM, Jang J, et al. High-resolution mapping of ventricular scar. *JACC: Clin Electrophysiol*. 2017;3(3):220-231.
5. Glashan CA, Tofig BJ, Tao Q, et al. Multisize electrodes for substrate identification in ischemic cardiomyopathy. *JACC: Clin Electrophysiol*. 2019;5(10):1130-1140.
6. Glashan CA, Beukers HKC, Tofig BJ, et al. Mini-, micro-, and conventional electrodes. *JACC: Clin Electrophysiol*. 2021;7(2):197-205.
7. Friedman BM, Dunn MI. Postinfarction ventricular aneurysms. *Clin Cardiol*. 1995;18(9):505-511.
8. Marchlinski FE, Callans DJ, Gottlieb CD, Zado E. Linear ablation lesions for control of unmappable ventricular tachycardia in patients with ischemic and nonischemic cardiomyopathy. *Circulation*. 2000;101(11):1288-1296.
9. Cano O, Hutchinson M, Lin D, et al. Electroanatomic substrate and ablation outcome for suspected epicardial ventricular tachycardia in left ventricular nonischemic cardiomyopathy. *JACC*. 2009;54(9):799-808.

10. Briceño DF, Romero J, Gianni C, et al. Substrate ablation of ventricular tachycardia: late potentials, scar dechanneling, local abnormal ventricular activities, core isolation, and homogenization. *Cardiac Electrophysiol Clin*. 2017;9(1):81-91.
11. Compagnucci P, Dello Russo A, Bergonti M, et al. Ablation index predicts successful ablation of focal atrial tachycardia: results of a multicenter study. *J Clin Med*. 2022;11(7):1802.
12. Casella M, Gasperetti A, Gianni C, et al. Ablation index as a predictor of long-term efficacy in premature ventricular complex ablation: a regional target value analysis. *Heart Rhythm*. 2019;16(6):888-895.
13. Josephson ME, Anter E. Substrate mapping for ventricular tachycardia. *JACC: Clin Electrophysiol*. 2015;1(5):341-352.
14. Cassidy DM, Vassallo JA, Marchlinski FE, Buxton AE, Untereker WJ, Josephson ME. Endocardial mapping in humans in sinus rhythm with normal left ventricles: activation patterns and characteristics of electrograms. *Circulation*. 1984;70(1):37-42.
15. Cassidy DM, Vassallo JA, Buxton AE, Doherty JU, Marchlinski FE, Josephson ME. The value of catheter mapping during sinus rhythm to localize site of origin of ventricular tachycardia. *Circulation*. 1984;69(6):1103-1110.
16. Glashan CA, Androulakis AFA, Tao Q, et al. Whole human heart histology to validate electroanatomical voltage mapping in patients with non-ischaemic cardiomyopathy and ventricular tachycardia. *Eur Heart J*. 2018;39(31):2867-2875.
17. Sramko M, Abdel-Kafi S, van der Geest RJ, et al. New adjusted cutoffs for "normal" endocardial voltages in patients with post-infarct LV remodeling. *JACC: Clin Electrophysiol*. 2019;5(10):1115-1126.
18. de Bakker JM, van Capelle FJ, Janse MJ, et al. Slow conduction in the infarcted human heart. 'Zigzag' course of activation. *Circulation*. 1993;88(3):915-926.
19. Frontera A, Melillo F, Baldetti L, et al. High-density characterization of the ventricular electrical substrate during sinus rhythm in post-myocardial infarction patients. *JACC: Clin Electrophysiol*. 2020;6(7):799-811.
20. Anter E, Li J, Tschabrunn CM, Nezafat R, Josephson ME. Mapping of a post-infarction left ventricular aneurysm-dependent macroreentrant ventricular tachycardia. *HeartRhythm Case Rep*. 2015;1(6):472-476.
21. Igarashi M, Nogami A, Kurosaki K, et al. Radiofrequency catheter ablation of ventricular tachycardia in patients with hypertrophic cardiomyopathy and apical aneurysm. *JACC: Clin Electrophysiol*. 2018;4(3):339-350.
22. Amin M, Farwati M, Hilaire E, et al. Catheter ablation of ventricular tachycardia in patients with postinfarction left ventricular aneurysm. *J Cardiovasc Electrophysiol*. 2021;32(12):3156-3164.
23. Nakahara S, Tung R, Ramirez RJ, et al. Distribution of late potentials within infarct scars assessed by ultra high-density mapping. *Heart Rhythm*. 2010;7(12):1817-1824.
24. Nakashima T, Cheniti G, Takagi T, et al. Local abnormal ventricular activity detection in scar-related VT: microelectrode versus conventional bipolar electrode. *Pacing Clin Electrophysiol*. 2021;44(6):1075-1084.

SUPPORTING INFORMATION

Additional supporting information can be found online in the Supporting Information section at the end of this article.

How to cite this article: Dello Russo A, Compagnucci P, Bergonti M, et al. Microelectrode voltage mapping for substrate assessment in catheter ablation of ventricular tachycardia: a dual-center experience. *J Cardiovasc Electrophysiol*. 2023;34:1216-1227. doi:10.1111/jce.15908